Lasers in Manufacturing Conference 2015

Effects of ultrashort laser ablation in copper and stainless steel

Wagner de Rossi[a]*, Denilson de Camargo Mirim[b], Nilson Dias Vieira Júnior[a] and Ricardo Elgul Samad[a]

[a]*Instituto de Pesquisas Energéticas e Nucleares- IPEN, Av. Lineu Prestes 2242 – Cidade Universitária - CEP: 05508-000 - São Paulo - SP BRAZIL*

[b]*Second affiliation, Address, City and Postcode, CountryInstituto Federal de Educação, Ciência e Tecnologia de São Paulo IFSP - Campus Avançado Sorocaba, Rua Maria Cinto de Biaggi 130 – CEP 18059-410 – Sorocaba - SP - Brazil*

Abstract

Precision machining with ultrashort laser pulses strongly depends on the relationship between process parameters and physical and metallurgical properties of the metal machined. This relationship, however, varies in the course of the process depending on the number of pulses that hit the same spot on the material being processed, and this need to be known and compensated for precision machining. This variation arises due to defects in the crystal lattice produced by the laser pulses. These defects are cumulative and their influence is described by the incubation effects. Thus, the relationship between the threshold fluency F_{th} and the number N of overlapping pulses is a fundamental condition to obtain controlled and precise ablation with ultrashort laser pulses.

By means of a method developed by the authors, the D-Scan (Diagonal Scan), this study acquired a great amount of experimental data that allowed obtaining many $F_{th} \times N$ curves. These curves were measured for pulsewidths of 25, 80 and 120 fs for both copper and stainless steel. The results show differences with respect to the temporal widths and even more significant variations between the two metals. Copper, presented a 25 fs single pulse ablation threshold of 0.80 J/cm^2, much greater than for stainless steel, which is 0.30 J/cm^2. The incubation factor for copper, 0.78 is smaller than that for stainless steel, which is 0.85. After N=1,000 pulses the two metals presented Fth of around 0,07 J/cm^2.

The D-Scan technique also allowed observing many different morphologies of the ablated region. The process parameters (fluency, N and temporal width) related to these morphologies could be easily determined in a clear and fast way. Therefore, the process conditions to obtain a specific surface structure as LIPSS, nanocones, fusion and fusion with phase explosion was determined to these two materials and the method can be used to any other kind of material.

Keywords: Micro processing; ablation; surface processing; femtosecond laser.

* Corresponding author. Tel.: +55-011-3133-9363; fax: +55-011-3133-9374.
E-mail address: wderossi@ipen.br.

1. Introduction

Ultrashort laser pulses with pulse widths around 100 fs and intensities in the range 1012-1014 W/cm^2 are generally used for ablation of solids. Because the duration of these pulses are shorter than the lattice ions vibrational period, most of the pulse energy is transferred to the material electrons, heating them without affecting the ions of the lattice. Most of this absorbed energy is then carried away with the ablated material and only a very small portion is coupled to the ions. The amount of heat produced at the lattice is so small that in practice, the heat-affected zone can be neglected and ablated surface is virtually free of melted material. These characteristics make ultrashort laser pulses very attractive for applications where high accuracy, integrity of the properties of the substrate and free of burrs finish are required.

In addition to these properties, the interaction of a femtosecond laser pulse with a surface of any type of material also has distinct characteristics depending upon the fluence used. Near the threshold can results in the formation of the so called “ripples”, or “Laser Induced Periodic Structures” (LIPSS), which are regularly aligned, long and periodic structures (Reif, Costache et al. 2009) (Barada and Mool 2010). Typical periodicity is smaller than the laser wavelength, and for enough number of pulses it can evolve to trenches as deep as one μm. The spacing and orientation of the ripples seems to depend mainly on the beam properties, as energy, number of shots, polarization and angle of incidence, and then, in principle can be controlled to some extent.

As the number of pulses or their fluence increase, the ripple pattern is broken by the formation of conical like structures, which present a typical feature size and spacing at the order of few micrometers or even smaller. These same structures can also be changed with the increase of fluence and number of superimposed pulses. For higher process efficiency, direct machining of larger preprogrammed structures requires high fluence pulses. This, however, can produce heat, melt and burrs, but the correct use of process parameter can minimize or virtually eliminate these drawbacks.

As seen, the choice of process parameters enables the control of the produced structure, which can roughly be divided in three type: ripples, cone-like and directly machined structures. Each of these structures has its practical applications and to find the right conditions for obtaining it can be a laborious task. In addition to the fluence and the number of superimposed pulses, the final characteristic of the processed surface may also depend on the duration and polarization of the laser pulse as well as the physical properties of the material.

This work uses the D-Scan method, introduced by the authors (Samad and Vieira 2006) (Samad, Baldochi et al. 2008), to find the appropriate process conditions for each of these structures for stainless steel VI 138 and pure copper. These two materials have very different thermal properties for which the temporal width of pulses can take an important hole in the results of micromachining.

2. Experimental work

In the D-Scan method used, a focused TEM_{00} Gaussian beam propagates (Z-axis) perpendicularly to the sample surface, which moves in Z and Y-axis at the same time. In a position near the beam waist, a profile is recorded as shown in Fig. (1). The ablation region has a minimum width in the focus position and two maximum lobes, with width $2\rho_{max}$, symmetrically located before and after the beam waist.

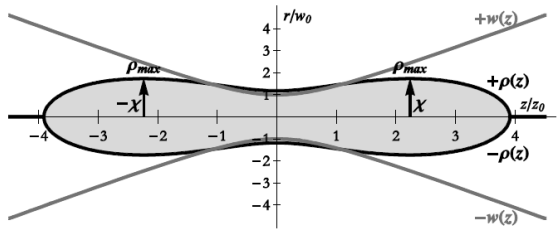

Fig. 1. Profile recorded on the sample surface having two lobes at maximum transverse position X with the maximum dimension $2\rho_{max}$. Lines + W (z) and W (z) represents the profile of the laser beam where the intensity is $1/e^2$ of the peak value.

Neglecting thermal effects, it was shown (Samad and Vieira 2006) that for a Gaussian TEM_{00} laser beam, the ablation threshold F_{th} is directly related to the pulse energy E_0 and maximum size ρ_{max}, through the relation:

$$F_{th} = \frac{E_0}{e\pi\rho_{max}^2} \cong 0.117\frac{E_0}{\rho_{max}^2}, \tag{1}$$

To take into account the effects of incubation, the overlay of N different pulses is regarded as the ratio of the sum of the intensities produced in (X, ρ_{max}) per pulse that impinges the sample during its movement, and the intensity of the pulse at (x, 0). On this basis, it can be shown, (de Rossi, Machado et al. 2012) (Machado, Samad et al. 2012) that:

$$N = \vartheta_3(0, e^{-\left(\frac{v_y}{f\rho_{max}}\right)^2}) \tag{2}$$

Where ϑ_3 is the theta of Jacobi elliptic function of the third kind; f is the laser repetition rate and ν_y is the sample translation speed in the Y-axis. For low speeds and low repetition rates, the eq. (2) can be approximated to:

$$N \sim 1.8\rho_{max}/\nu_y, \tag{3}$$

The materials used in this investigation were copper and stainless steel VI 138. The large difference in the thermal properties of materials can provide a good indication of the influence of the temporal width of the laser pulses both in the removal of the material and in the conduct of heat out of the irradiated area. In addition to the very different thermal properties compared to copper, the choice of stainless steel VI 138 was due to the great interest in its use in surgical implants. In these cases, micromachining and marking must result in surfaces free of significant changes in its structural or physic-chemical properties.

The materials have their thermal properties shown in Table (1). Samples with 1 mm thickness were embedded in Bakelite, ground and polished with 3μm granulation diamond paste.

The experiment was conducted with a Ti: Sapphire laser system (Femtopower Compact Pro EC-Phase HP/HR Femtolasers) with emission centered at 785 nm, bandwidth of 37 nm, linearly polarized in the horizontal direction (Y-axis) and maximum repetition rate of 4 kHz. Three different temporal pulse durations were used: 25, 80 and 125 fs. The energies of the pulses were attenuated to approximately 90 μJ, a lens of focal length of 75 mm focused the beam and the sample was driven by a 3-axis computer controlled system.

Table 1. Thermal characteristics of the materials.

Material	Fusion point (°C)	Coefficient of linear thermal expansion (10-6/°C)	Thermal conductivity (W/m - K)	Specific heat (J/Kg - K)
Copper	1083	17,7	398	386
VI 138 steel	1500	16	15,9	502

In all experiments, the sample was moved from a position in which the focus was above the surface to a position where the focus was inside the sample.

Many different repetition rates and traverse speeds (in Y-axis) were combined to cover overlays since a single pulse to thousands of pulses. The velocities of longitudinal and transverse displacement of the sample, ν_x and ν_y were always equal to generate elongated profiles (Samad and Vieira 2006). After recording of each D-scan trace, the sample was moved vertically (X direction) by 400 microns, the separation was used as calibration to measure the maximum 2ρ in an optical microscope. Figure (2) shows traces obtained in the experiment with 25 fs pulses.

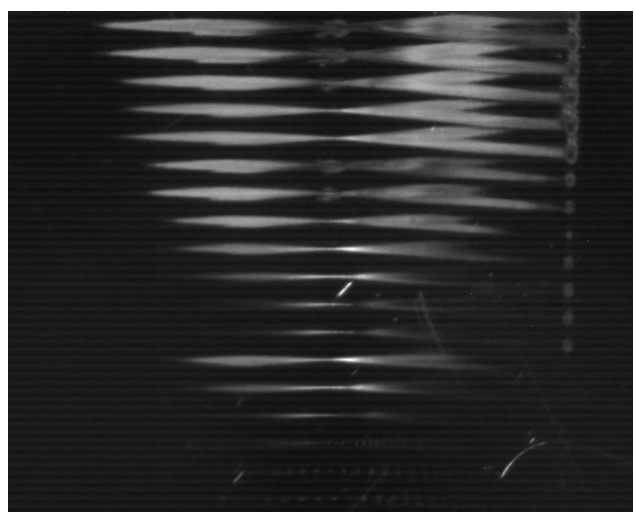

Fig. 2. Traces generated by the D-Scan technique in steel VI 138, with 25 fs laser pulses.

The central, narrow part of Figure 2 corresponds to focus on the surface. The left mark was produced with the focus within the workpiece while the right side was made with the focus away from the surface. It shows a deformation in the features of the etched traces in the right side; this must have been caused by a scattering of the laser beam produced by the plasma in the air at the focal position. For this reason, the width 2ρmax was only measured in the left side of Fig.2.

The width $2\rho_{max}$ of each of these traces was used to evaluate F_{th} as function of the number N of overlapping pulses. The curve interpolation settings for Fth x N, gives the incubation parameter (k) which

depends on the incubation model used. Furthermore, analysis of features of each portion in different traces provides the experimental conditions for obtaining each of the three machining morphologies described above. All irradiations were accomplished in protective atmosphere of argon, and in sequence, samples were cleaned with isopropyl alcohol in an ultrasonic device to remove debris from the ablation deposited.

Figure 3 shows the image taken using scanning electron microscope to the first six more intense scratches generated by the use of D-Scan technique with stainless steel VI 138. The pulselenght is 25 fs and scanning speeds increase from top to bottom. The figure on the right shows the position where $2\rho_{max}$ were measured.

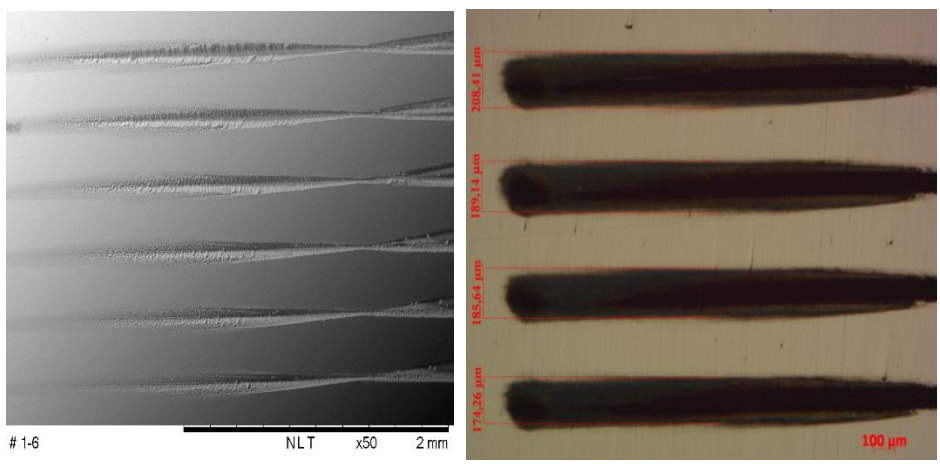

Fig. 3. In the left, SEM image showing the six more deep grooves generated by the D-Scan technique in VI 138 steel. In the right, OM image shows where $2\rho_{max}$ where measured.

The $2\rho_{max}$ values were measured for all cases and the ablation threshold $F_{th}(N)$ as a function of the number N of overlapped pulses was calculated according to the expression (4) (Jee, Becker et al. 1988) for each experimental condition. Figure 4 shows plots of F x N in a log x log scale for both materials and for the three temporal pulse length used. The solid lines show a fit of the data considering the incubation model for metals (Jee, Becker et al. 1988) given by:

$$F_N = F_1 N^{k-1} \tag{4}$$

Using Eq. (4), the K factor adjustment used to obtain the solid lines in figure 4 provides the incubation parameter for the material. It is seen a steady decrease in F_{th} with the increase in N for both, stainless steel and copper. The same behavior remains even with pulsewidth variation. Although the behavior is similar for the two materials, copper presents higher values of $F_{th}(N)$ for low overlapping rates when compared to stainless steel. It is also clear a faster decrease of F_{th} for copper than for stainless steel. The temporal pulsewidths in the used range seem not to play an important role in the ablation threshold. Only a small increase in $F_{th}(N)$ for low overlap rates seems to occur for copper.

These observed phenomena, reflect not only the greatest difficulty in the copper ionization (for one or few pulses), due to its higher conductivity, but also indicates a greater susceptibility to damage that reduce the mobility of free electrons with the accumulation of pulses. In fact, after an accumulation of more than 1000 pulses, copper ablation threshold is similar or even lower than that of stainless steel.

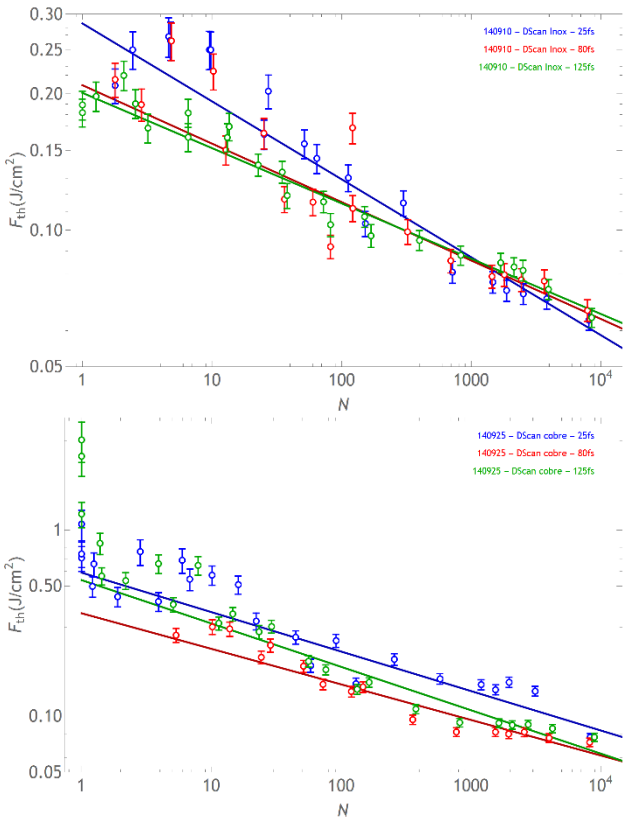

Fig. 4. Ablation thresholds (F_{th}) X number of overlapping pulses (N) for stainless steel VI 138 (up) and copper (down).

Analysis of the features of the different regions in the various etched scratches allowed defining a set of process parameters to obtain three very distinct morphologies for each material. In the first condition, with few pulses, takes place the formation of small periodic ripples on the surface, the LIPPS. With increasing number of pulses, the second condition occurs where LIPPS are deepened and broken to give rise to a granular structure. Finally, the large accumulation of pulses leads to a third condition where a more effective machining with higher material removal takes place. These three conditions were not observed at the focus, but at the same location where $2\rho_{max}$ were measured.

For stainless steel VI 138, the formation of Lipps is observed since a single pulse up to about 50 pulses. The period of the structures is about 600 nm and does not change with increasing of overlapping pulses. In the case of copper, the formation of LIPPS is only observed after superposition of 10 pulses, remaining present even after an overlapping of 130 pulses, figure (5).

The intermediate condition, with grainy structure formation, occurs with overlapping between 45 and 720 pulses for stainless steel and between 600 and 2000 pulses for copper Fig. (6). Morada et al (MOrada, S. et al. 2013) shown similar result in the study of roughness super-hydrophobicity for 316L stainless steel.

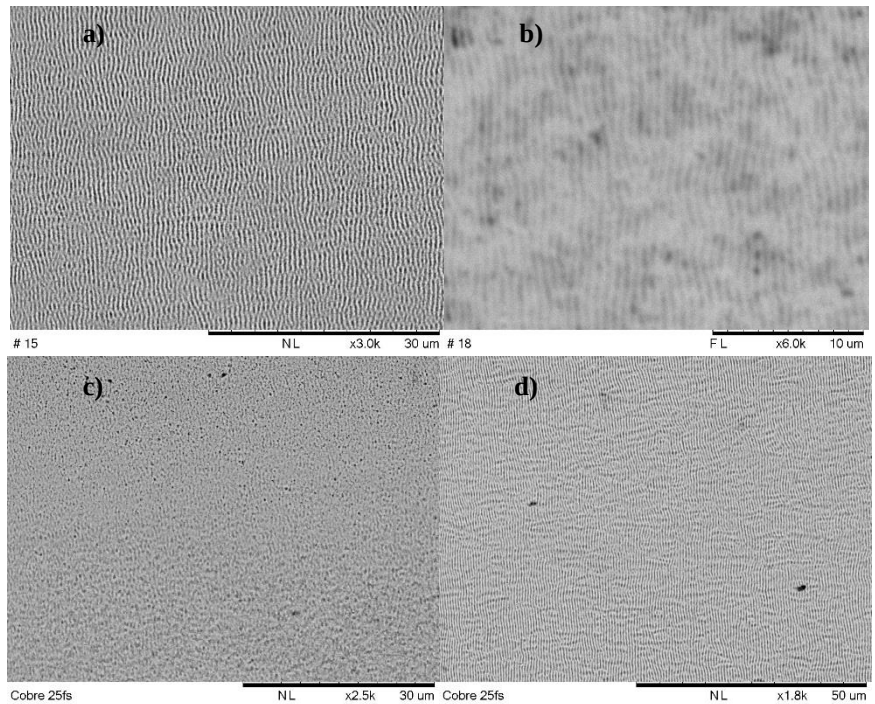

Fig. 5. LIPSS on VI 138 steel and copper. N = 9 pulses (a) and N = 1.7 (b) for steel. N = 10 (c) and N = 130 (d) for copper.

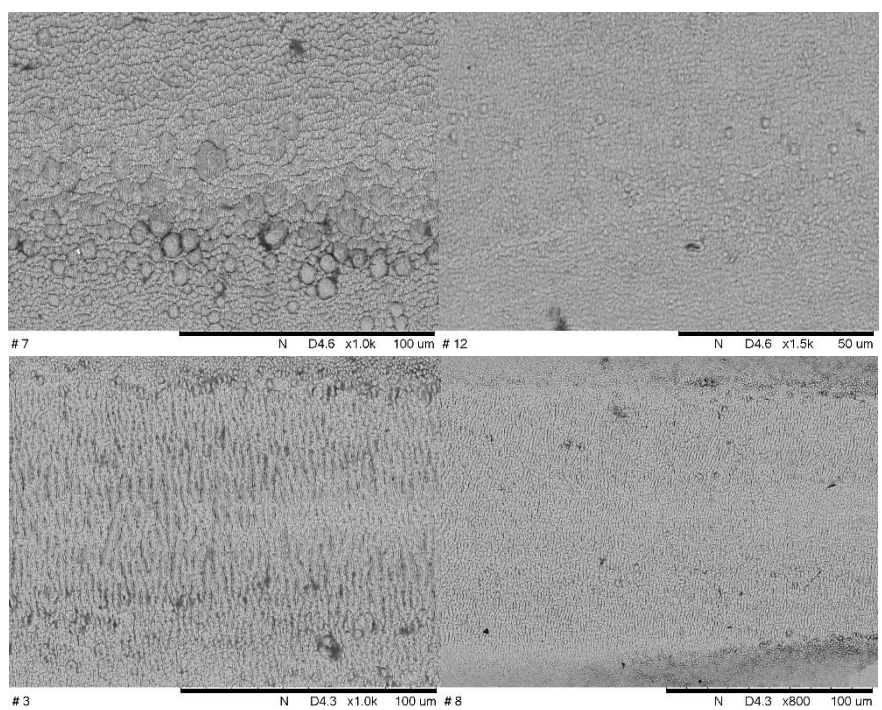

Fig. 6. Grainy structure obtained in VI 138 steel (above) and copper (below).

The most severe condition with greatest material removal arises by the overlap of about 1400 to 16100 pulses for stainless steel and between 3100 and 16700 pulses for copper.

The most severe condition, with greatest material removal, arises after the overlap of about 1400 to 16100 pulses for stainless steel and between 3100 and 16700 pulses for copper.

Figure 7 shows the traces produced on the sample of VI 138 steel with the largest overlapping pulses. Contrary to what one might expect, it is observed that the region where the focus is on the sample surface does not correspond to the greater depth of ablation. This fact is also repeated for less overlapping conditions and for copper. With greater intensity at focus, it was expected a higher material removal and greater machining depth at this point. One factor that may have contributed to this decrease in the removal of material is the big and dense plasma produced at this point. In adjacent points, the lowest intensity does not produce a so intense plasma and absorption and scattering of the laser beam are reduced.

The removal efficiency is higher when there is no plasma and the scanning of laser beam out of focus position produces a figure where the ablation depth reaches a maximum and then decreases gradually until no ablation occurs. Detailed study of the relationship between intensity and material removal is being studied and should result in an optimization of processes with ultrashort pulse lasers in both metals. With similar process conditions, the morphology of the traces obtained in stainless steel shows more elongated and deep profile, Fig. 7a and 7b than in copper Fig. 7c. This means a process that is more efficient with bigger amount of material removal in the less conductive metal.

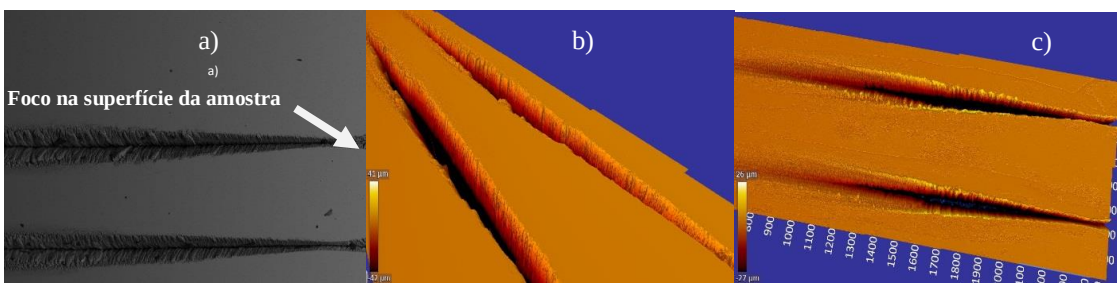

Fig. 7. Grooves machined with larger overlapping pulses in VI 138 steel (a), (b) and copper (c).

From the observation in the scratches produced in both materials, the better edge finish was obtained with the pulsewidth of 25 fs. In copper the best ablation and finish condition, occurred with overlap of N ~ 3100 pulses. In stainless steel the most favorable condition was for N ~ 1450 overlapping pulses, Fig. (8).

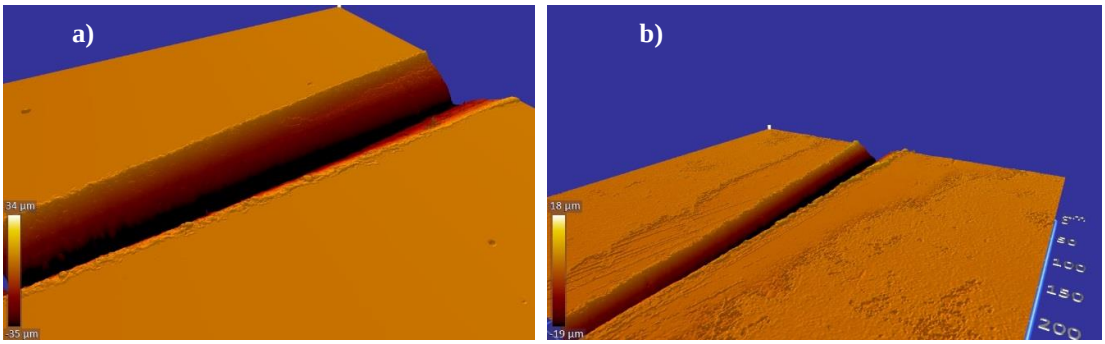

Fig. 8. Grooves machined with best condition in which the rim is better defined, VI 138 steel (a) and Cu (b).

At higher intensity condition close to focus, and most overlapping pulses, no change was observed in the morphology of the grains for both copper and for stainless steel. Figure 9 displays the cutting edge for copper that, with the used magnification, did not show any effect of heat in its vicinity.

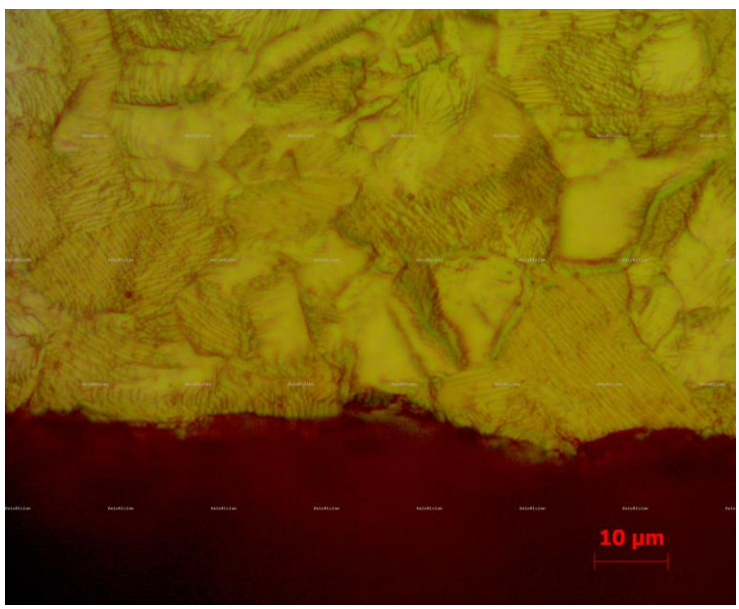

Fig. 9. Cutting edge for copper with no evidence of thermal effects.

3. Conclusion

Using the D-Scan technique it was possible to get many different morphologies on the surfaces of steel VI 138 and copper. Obtained data showed that the ablation threshold (F_{th}) decreases in a similar manner to the three temporal pulsewidths studied as function of overlapping pulses, for both materials. Comparing the results obtained in the VI 138 and copper, it was found that in similar conditions of process, the machined profiles are deeper and more elongated in steel while are shorter and shallower in copper. It was also possible to identify three different morphologies ablation on the surface of both materials. At VI 138, there

was a more severe ablation between 1400 and 16100 overlapping pulses , while in copper this occurred between 3100 and 16700 overlapped pulses. A granular formation occurred between 60 and 720 pulses in the steel and between 600 and 2000 overlapped pulses on the copper. The formation of periodic undulations occurred between 1 and 50 pulses in the steel and between 10 and 130 superimposed pulses on the copper. In the latter condition occurs a smooth ablation of a surface layer with some darkening, showing the possibility of use of these parameters for marking on the surface of these materials. Hence, similar morphological ablation patterns can be obtained for both materials, but in different fluences and different number of overlapping pulses.

It was also found that, as the time width of the pulses is reduced there is an improvement on the edges of the grooves, and pulse length of 25 fs is the most suitable for producing precise cuts in both materials.

The ultrashort pulse laser ablation in VI 138 steel, and copper, produced different morphologies with different process parameters showing promising results, which may be used in micromachining, recording and marking of these materials.

Acknowledgements

This research was supported by CNPq under contract 310111/2009-9.

References

Barada, K. N. and C. G. Mool, 2010. Ultrafast laser-induced self-organized conical micro/nano surface structures and their origin. Optics and Lasers in Engineering. **48:** 966-973.

de Rossi, W., L. M. Machado, N. D. Vieira Jr and R. E. Samad, 2012. "D-Scan Measurement of the Ablation Threshold and Incubation Parameter of Optical Materials in the Ultrafast Regime." Physics Procedia **39**: 642-649.

Jee, Y., M. F. Becker and R. M. Walser, 1988. "Laser-induced damage on single-crystal metal surfaces." Journal of the Optical Society of America B-Optical Physics **5**(3): 648-659.

Machado, L. M., R. E. Samad, W. de Rossi and N. D. Vieira Junior, 2012. "D-Scan measurement of ablation threshold incubation effects for ultrashort laser pulses." Optics Express **20**(4): 4114-4123.

MOrada, M., K. S., P. Englezos and G. S. Hatzikiriankos, 2013. Femtosecond laser irradiation of metallic surfaces: effcts of laser parameters on superhydrophobicity. Nanotecnology**:** 24.

Reif, J., F. Costache, O. Varlamova, G. Jia and M. Ratzke, 2009. "Self-organized regular surface patterning by pulsed laser ablation." physica status solidi (c) **6**(3): 681-686.

Samad, R. E., S. L. Baldochi and N. D. Vieira Jr, 2008. "Diagonal scan measurement of Cr:LiSAF 20 ps ablation threshold." Applied Optics **47**(7): 920-924.

Samad, R. E. and N. D. Vieira, 2006. "Geometrical method for determining the surface damage threshold for femtosecond laser pulses." Laser Physics **16**(2): 336-339.